Kinetik: Game Technology, Information System, Computer Network, Computing, Electronics, and Control
Journal homepage: http://kinetik.umm.ac.id
ISSN: 2503-2267
Vol. 11, No. 2, May, Pp. 259-272

An adaptive cross-tied interconnection for shaded PV arrays: a mathematical analysis for efficiency enhancement

Efendi S Wirateruna*[1], Mohammad Jasa Afroni[1], Wahyu Mulyo Utomo[1], Mukhammad Zakky Syahrul Aziz[2]
Departement of Electrical Engineering, Faculty of Engineering, Universitas Islam Malang, Malang, Indonesia[1]
Department of Electrical Engineering, Faculty of Electrical and Electronics Engineering, Universiti Tun Hussein Onn Malaysia, Johor, Malaysia[2]

Article Info
Keywords:
PV Farm, Partial Shading Condition, ACTI Technique, Global Maximum Power Point, Series-Parallel Configuration

Article history:
Received: October 12, 2025
Accepted: January 27, 2026
Published: May 01, 2026

Cite:
E. S. Wirateruna, M. J. Afroni, W. M. Utomo, and M. Z. S. Aziz, "An Adaptive Cross-Tied Interconnection for Shaded PV Arrays: A Mathematical Analysis for Efficiency Enhancement", *KINETIK*, vol. 11, no. 2, May. 2026.
https://doi.org/10.22219/kinetik.v11i2.2529

*Corresponding author.
Efendi S Wirateruna
E-mail address:
efendi.s.wirateruna@unisma.ac.id

Abstract
This study investigates the Adaptive Cross-Tied Interconnection (ACTI) configuration to improve the power output efficiency of photovoltaic (PV) arrays operating under partial shading conditions. The objective of this study is to develop a mathematical formulation that describes the behavior of ACTI compared to the conventional Series-Parallel (SP) configuration. Mathematical modeling is used to analyze the current distribution, voltage relationships, and the effect of shading patterns on the total output power. Simulations are performed using MATLAB/Simulink to verify the theoretical analysis results. This adaptive configuration dynamically adjusts the cross-tied interconnections based on the illumination intensity data, thereby balancing the current between shaded and non-shaded modules. The results show that ACTI successfully reduces current mismatch losses and increases output power without increasing circuit complexity. In a 3×3 PV array, the ACTI configuration yields a power increase of up to 48% compared to the SP configuration. In a 5×5 array, the efficiency increases ranges from 2% to 6%, depending on the shading pattern. The adaptive switching strategy maintains the current flow stability and produces a smoother power-voltage curve, enabling faster and more accurate tracking of the global maximum power point. These results demonstrate that ACTI provides an efficient, economical, and mathematically sound solution for improving the performance of PV systems under non-uniform irradiation conditions.

1. Introduction

Electrical energy is a vital resource that is essential for modern human needs. The demand for electrical energy continues to increase with growing population activity, which is one of the contributing factors to rising pollution and global warming, as this energy largely comes from fossil fuels such as coal and petroleum, which are continuously exploited and decreasing in availability each year [1], [2]. The use of renewable energy is one solution to reduce the impact of increasing pollution and global warming. One of the renewable energy sources is solar energy. Solar energy can be utilized as an alternative energy source without producing pollution during operation, making it an attractive solution for mitigating global warming. Photovoltaic (PV) systems are among the most widely used renewable energy technologies, producing distinctive power characteristic [3]. Accordingly, numerous researchers have focused on advancing technologies aimed at maximizing the optimal deployment of PV systems to meet growing energy demands.

However, PV panels face efficiency issues when operating under partial shading conditions or rapid changes in irradiance [4], [5]. Under ideal conditions, PV systems exhibit a power-voltage (P-V) characteristic curve with a single maximum power peak [6]. Partial shading conditions are often caused by clouds, dust, or objects obstructing the surface of the solar panel. This condition can lead to a reduction in maximum power output and the emergence of multiple peaks (local and global) in the P-V curve. Therefore, PV array configuration techniques that can mitigate the effects of partial shading conditions (PSC) are crucial for improving energy efficiency.

In general, there are several types of PV array configurations, namely Series, Parallel, Series-Parallel (SP), Honeycomb (HC), Bridge-Link (BL), and Total-Cross-Tied (TCT) connections. Among these configurations, the TCT configuration shows the best performance and highest power output, especially under PSC conditions [7], [8], [9], [10]. However, TCT requires a large number of cross-connections, resulting in implementation complexity and high hardware costs, particularly in large-scale systems. Conversely, the SP configuration is simpler and widely used in practice, but its performance is less than optimal when dealing with PSCs. This situation highlights the need for new configuration methods that strike a balance between implementation simplicity and efficiency improvement.

In [11], [12], the SP configuration was used for PV farm optimization under PSC. The measurement method involved monitoring the voltage of each string, which was then clustered into three groups—full, medium, and low irradiation—using a fuzzy algorithm. Clustering occurs when differences in voltage values between strings indicate the

presence of PSC. Each cluster is connected to a separate Maximum Power Point Tracking (MPPT) unit and inverter [13], [14]. However, this method is still based on a group-level approach and does not detect PSC in detail.

A subsequent development in configuration methods involves adding switching control between strings and dynamically changing the configuration when PSC are detected [15]. The PV array size used in the simulation was a 4×4 PV array with a TCT configuration. The interconnections between columns 1 and 2, as well as columns 3 and 4, are dynamically adjusted during switching. The PSC detection method involves evaluating the actual power output [16], [17], [18]. If the power difference exceeds 10%, PSC is indicated, triggering the switching unit to reconfigure the interconnections electrically.

Some researchers have employed population-based algorithms [19], [20], [21], [22], [23], such as the Particle Swarm Optimization (PSO), Genetic Algorithm (GA), and Dragonfly Algorithm. These techniques are highly complex because each module is reconfigured; although the physical position remains unchanged, the electrical connections are rearranged by the AI algorithms. The AIalgorithms search for the optimal configuration when PSC is detected. While this approach is effective in quickly identifying configurations that maximize energy generation, the required switching and control infrastructure becomes increasingly expensive as the PV array size grows.

Various PV array configuration and reconfiguration techniques have been proposed to enhance output power under partial shading conditions; however, they still face practical implementation challenges. Series–Parallel configurations offer a simple structure but are highly vulnerable to current mismatch. In contrast, Total Cross-Tied, static reconfiguration, and AI-based adaptive methods require extensive wiring, numerous switching devices, and complex, costly control systems, limiting their feasibility for large-scale PV installations. These methods primarily focus on improving power through interconnection reconfiguration but have yet to achieve a balanced solution that combines enhanced power performance with implementation simplicity. This situation highlights the need for approaches that effectively boost power output under partial shading while minimizing system complexity and interconnection requirements.

As a solution, Adaptive Cross-Tied Interconnection (ACTI) was introduced. Unlike fixed TCT configuration, ACTI employs an adaptive cross-tied scheme with fewer connections while still achieving balanced current distribution. By selecting appropriate cross-connection points, ACTI can reduce mismatch losses without introducing excessive complexity. Furthermore, ACTI can be formulated mathematically, enabling quantitative analysis of the effect of shading patterns on current distribution and output power. This mathematical analysis provides a deeper understanding of the relationship between array configuration, shading conditions, and improvements in power efficiency.

The main novelty of this research lies in the mathematical formulation that explicitly analyzes the effects of adding and removing cross-tied lines on the current distribution, I–V characteristics, and the potential to increase the global power output of the PV array under partial shading conditions. This formulation is used not only to validate the simulation results but also as a theoretical basis for determining the optimal placement of cross-tied lines without excessively increasing wiring complexity. Based on this foundation, the Adaptive Cross-Tied Interconnection (ACTI) configuration is proposed as a practical solution that significantly increases power compared to the Series–Parallel configuration and achieves performance comparable to Total Cross-Tied, while using a minimal number of interconnections, particularly under static partial shading conditions.

2. Mathematical Analysis of PV array

2.1 PV Array Modelling

The photovoltaic module can be represented by an equivalent circuit. Figure 1 depicts the the single-diode equivalent circuit of a photovoltaic module, which consists of a current source, a parallel diode, series resistance (R_s), and parallel resistance (R_p). The output current equation is expressed in Equation 1.

$$\mathrm{I} = \mathrm{I_{ph}} - \mathrm{I_s}\left[\mathrm{e}^{\mathrm{q}\left(\frac{\mathrm{V_{pv}+IR_s}}{\mathrm{b.k.T}}\right)} - 1\right] - \left(\frac{\mathrm{V_{pv}} + \mathrm{IR_s}}{\mathrm{R_p}}\right) \quad (1)$$

Where I_s is the saturation current; I_{ph} is the photocurrent generated by photons; V_{pv} is the photovoltaic voltage; q is the electron charge ($1.6 \times 10^{-19}\ C$); I is the output current of the panel; k is the Boltzmann constant; T is the cell temperature in Celsius; b is the diode ideality factor [24], [25]. PV module parameters can be obtained from experiments or datasheets. Temperature and irradiance are the most important parameters in determining curve features.

$$\mathrm{I_{ph}} = \mathrm{I_{ph,std}}(1 + \mathrm{C_i}\Delta\,\mathrm{T})\frac{\mathrm{S}}{\mathrm{S_{std}}} \quad (2)$$

$$I_s = \frac{I_{sc,std} + C_i \Delta T}{\exp\left(\frac{V_{oc,std} + C_v \Delta T}{b\, V_t}\right) - 1} \quad (3)$$

Equation 2 describes the output current generated by the photons. Where $I_{ph,typ}$ is the photocurrent generated under standard test conditions, namely irradiance of 1000 W/m^2 and temperature 25° C. S and S_{std} represent the module irradiance and the standard irradiance (1000 W/m^2), respectively. The saturation current is expressed by Equation 3 [24]. C_v is the temperature coefficient of the short circuit current, while C_i is the temperature coefficient of the open-circuit voltage. $V_{oc,typ}$ and $I_{sc,typ}$ denote the open-circuit voltage and short-circuit current, respectively under standard test condition. Furthermore, $\Delta T = T - T_{STC}$, where T and T_{STC} represent the actual temperature and the temperature at standard test conditions (in Kelvin), respectively.

2.2 Mathematical analysis of TCT configuration

This chapter begins by emphasizing the need for mathematical analysis to understand the behavior of a Total Cross-Tied (TCT) circuit under partial shading conditions. Each photovoltaic module is modeled using the single-diode approach, as this model accurately describes the current–voltagecharacteristics. In this model, the output current of the solar cell is determined by its photocurrent, reverse saturation current, and terminal voltage while considering temperature effects.

The chapter then explains how the interconnection of modules within an array produces specific equilibrium equations. In a TCT configuration, parallel nodes have equal voltage, while series paths carry equal current. This enables the derivation of equations for the total current and voltage of the array. The equations for the individual modules are first derived and then interconnected using Kirchhoff's laws. This mathematical approach provides the basis for analyzing various shading patterns. The simplest case begins with a single shaded module. From this case, the equations for the total current and total voltage of a 2×2 TCT array are derived. These equations demonstrate how reduced irradiance on a single module affects the current and voltage distribution of the entire array.

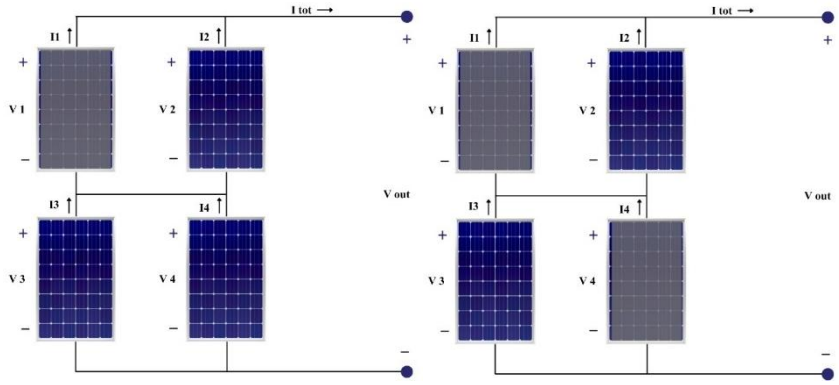

Figure 1. TCT Configurations for a 2×2 PV Array Under Partial Shading Conditions

Based on Kirchhoff's laws, as shown in Figure 1, the TCT configuration illustrates the relationship between the total voltage and total current, along with the voltage and current values of each PV module, as expressed in Equations 4 and 5.

$$I_{total} = I_1 + I_2 = I_3 + I_4 \quad (4)$$

$$V_{total} = V_1 + V_3 = V_2 + V_4 \quad (5)$$

A photovoltaic in a PV array configuration experiencing shading is characterized by a shading factor, β, as described in Equation 6 [19]. The shading ratio affects the total current generated by the PV module or PV array.

$$\beta = 1 - S_{sh}/S_c \quad (6)$$

Where S_{sh} represents the irradiance value under the shading conditions, and S_c denotes the incoming irradiance value. The mathematical equation analysis focuses on a diagonal irradiance model. The first condition considers one-shaded PV module, while the second condition considers two PV modules subjected to diagonal shading. An ideal assumption

is adopted in which the influence of the very small series resistance (R_s)and the very large parallel resistance (R_p) on the total current is negligiblecompared to the current variation caused by shading. Therefore, Equation 1 can be simplified into Equation 7.

$$\mathrm{I} = \mathrm{I_{ph}} - \mathrm{I_s}\left[\mathrm{e}^{\frac{\mathrm{qV_{pv}}}{\mathrm{bkT}}} - 1\right] \tag{7}$$

Figure 1(a) illustrates the first condition, in which one module is subjected to shading. The current for each module is calculated using Equations 8 and 9, derived from Equation 7. Here, S represents the nominal irradiance value 1000W/m^2.

$$I_1 = I_{ph} - \frac{\beta S_c}{S}.I_{ph} - I_s\left[\mathrm{e}^{\frac{\mathrm{qV_{pv}}}{\mathrm{bkT}}} - 1\right] \tag{8}$$

$$I_{2,3,4} = I_{ph} - I_s\left[\mathrm{e}^{\frac{\mathrm{qV_{pv}}}{\mathrm{bkT}}} - 1\right] \tag{9}$$

The total current is obtained by substituting Equations 8 and 9 into Equation 4. The relationship between the total current and voltage is expressed in Equation 10.

$$I_{total} = 2I_{ph} - \frac{\beta S_c}{S}.I_{ph} - 2I_s\left[\mathrm{e}^{\frac{\mathrm{qV_2}}{\mathrm{bkT}}} - 1\right] \tag{10}$$

Based on Equation 5, V_3 can be substituted into Equation 10 to obtain Equation 11.

$$I_{total} = 2I_{ph} - \frac{\beta S_c}{S}.I_{ph} - 2I_s\left[\mathrm{e}^{\frac{\mathrm{q(V_{total}-V_4)}}{\mathrm{bkT}}} - 1\right] \tag{11}$$

From Equations 4 and 5, where $V_3 = V_4$, the relationships between current and voltage, I_{total} and V_4 are expressed in Equations 12 and 13.

$$I_{total} = 2I_{ph} - 2I_s\left[\mathrm{e}^{\frac{\mathrm{qV_4}}{\mathrm{bkT}}} - 1\right] \tag{12}$$

$$V_4 = \frac{bkT}{q}Ln\left(\frac{2I_{ph} - I_{total} + 2I_s}{2I_s}\right) \tag{13}$$

Therefore, Equation 13 is subsequently substituted into Equation 11 to derive the relationship between total current and total voltage, as given in Equation 14.

$$I_{total} = 2I_{ph} - \frac{\beta S_c}{S}.I_{ph} - 2I_s\left[\mathrm{e}^{\left(\frac{qV_{total} - bkTLn\left(\frac{2I_{ph}-I_{total}+2I_s}{2I_s}\right)}{bkT}\right)} - 1\right] \tag{14}$$

The following analysis considers the Series-Parallel configuration for the first condition. The current value in the shaded string is the same as that expressed in Equation 8, while the current in the unshaded string is given by Equation 9, with V_{pv}=V_{total}. Thus, the total current in Equation 15 is obtained based on Equation 4.

$$I_{total} = 2I_{ph} - \frac{\beta S_c}{S}.I_{ph} - 2I_s\left[\mathrm{e}^{\frac{\mathrm{qV_{total}}}{\mathrm{bkT}}} - 1\right] \tag{15}$$

The second condition involves diagonal partial shading on the PV array, as shown in Figure 1 (b). The current equation for each module can be determined based on Equation 4.

$$I_{2,3} = I_{ph} - \frac{\beta S_c}{S}.I_{ph} - I_s\left[e^{\frac{qV_{pv}}{bkT}} - 1\right] \quad (16)$$

$$I_{1,4} = I_{ph} - I_s\left[e^{\frac{qV_{pv}}{bkT}} - 1\right] \quad (17)$$

Given the relationship $V_1 = V_2$, substituting Equations 16 and 17 into Equation 4 yields the total current equation as a function of voltage V_1, as formulated in Equation 18.

$$I_{total} = I_1 + I_2 = 2I_{ph} - \frac{\beta S_c}{S}.I_{ph} - 2I_s\left[e^{\frac{q(V_1)}{bkT}} - 1\right] \quad (18)$$

$$V_1 = \frac{bkT}{q} Ln\left(\frac{2I_{ph} - \frac{\beta S_c}{S}.I_{ph} - I_{total} + 2I_s}{2I_s}\right) \quad (19)$$

Based on Equations 4 and 5, with $V_3 = V_4$, the total current equation for row 2 is obtained in Equation 20.

$$I_{total} = I_3 + I_4 = 2I_{ph} - \frac{\beta S_c}{S}.I_{ph} - 2I_s\left[e^{\frac{q(V_3)}{bkT}} - 1\right] \quad (20)$$

$$I_{total} = 2I_{ph} - \frac{\beta S_c}{S}.I_{ph} - 2I_s\left[e^{\frac{q(V_{total}-V_1)}{bkT}} - 1\right] \quad (21)$$

Substituting Equation 19 into Equation 21, the relationship between total current and total voltage can be derived, as expressed in Equation 22.

$$I_{total} = 2I_{ph} - \frac{\beta S_c}{S}.I_{ph} - 2I_s\left[e^{\left(\frac{qV_{total} - bkTLn\left(\frac{2I_{ph} - \frac{\beta S_c}{S}.I_{ph} - I_{total} + 2I_s}{2I_s}\right)}{bkT}\right)} - 1\right] \quad (22)$$

The following analysis considers the Series-Parallel configuration for the second condition. When one of the modules in a string experience shading, the string current decreases to the current of the weakest module because, in a series configuration, the current must remain identical across all modules, making the shaded module the current-limiting element. The current values in both shaded strings are represented by Equation 16, with V_{pv}=V_{total}. Thus, the total current shown in Equation 23 can be obtained based on Equation 4.

$$I_{total} = 2I_{ph} - 2.\frac{\beta S_c}{S}.I_{ph} - 2I_s\left[e^{\frac{qV_{total}}{bkT}} - 1\right] \quad (23)$$

3. The Proposed Technique

A simulation-based approach is employed to analyze the performance of a photovoltaic (PV) array system under partial shading conditions by implementing an Adaptive Cross-Tied Interconnection (ACTI) configuration based on local block evaluation. All modeling is conducted using MATLAB/Simulink 2023b, which monitors the irradiance data of each PV module and activates automatic switches according to the specified control logic. The simulation utilizes a PV array with an initial Series-Parallel (SP) configuration as the baseline. Multiple static partial shading patterns are modeled for each PV array, representing shadows caused by buildings, trees, and accumulated dirt.

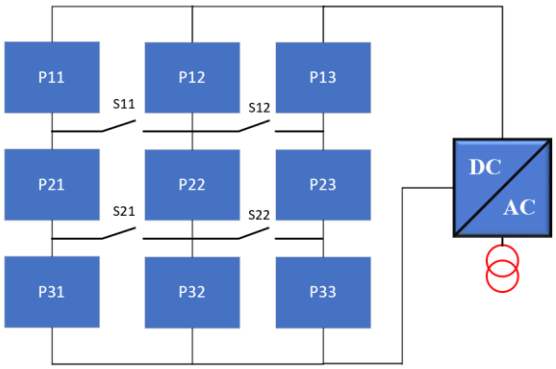

Figure 2. Adaptive Cross-tied Interconnection

A photovoltaic (PV) array configured in a Series-Parallel arrangement incorporates cross-tied interconnection paths between rows, which are linked through controlled switches, as illustrated in Figure 2. These switches are represented in Simulink using controlled switch blocks that operate in ON (connected) and OFF (disconnected) states. Under uniform irradiation conditions, all switches remain in the OFF state, causing the PV array function as a standard Series-Parallel configuration. When irradiation becomes non-uniform, specific switches are activated based on the control system's evaluation. In a 3×3 PV array, adaptive switches (S_{11}, S_{12}, S_{21}, S_{22}) are used, with each switch connecting a local block of 2×2 modules.

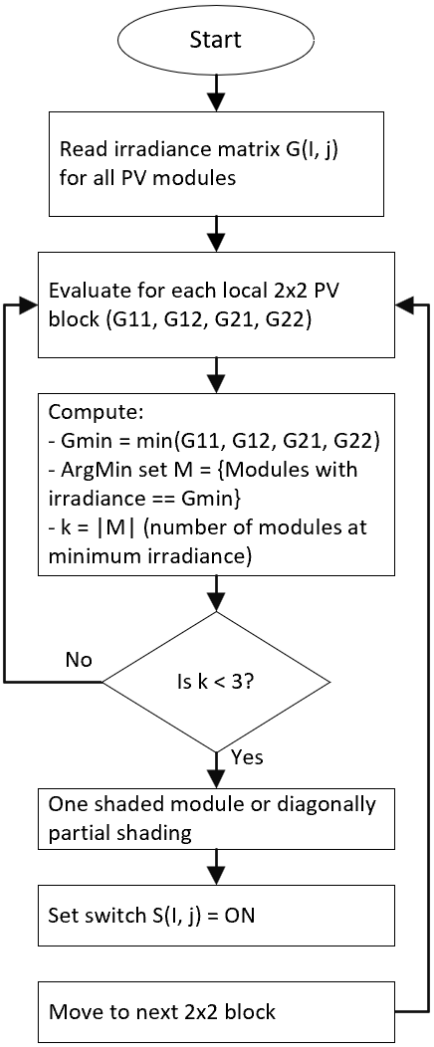

Figure 3. The Proposed Technique Flowchart

Figure 3 illustrates the operation of the ACTI technique for various PV array sizes, while the PV module specifications are presented in Table 1. Each switch $S_{i,j}$ connects four adjacent PV modules to form a 2×2 block. The system uses the ACTI flowchart algorithm to determine the operating state of each switch. The adaptive cross-tied method initiates its decision-making process by measuring the irradiance of each photovoltaic (PV) module within a 2×2 local block. The system identifies the minimum irradiance value (G_{min}) and counts the number of modules at this level, denoted as k. The value of k determines the switch configuration. When only one module exhibits the minimum irradiance ($k = 1$), the system identifies a single-module shading condition and activates the corresponding $S_{i,j}$ switch to allow current from the remaining modules to flow through the cross-link path, thereby reducing current mismatch losses.

Table 1. The PV Module specifications

The current of short circuit (A), I_{SC}	1.5
The voltage of open circuit (V), V_{oc}	22
The voltage at the maximum power point (V), V_{mpp}	18.5
Current at the maximum power point (A), I_{mpp}	1.2
Total number of cells	60
Cell Temperature (DegC)	25
Maximum Power Point (MPP)	22.2

If two modules exhibit the lowest irradiance ($k = 2$), the system classifies this condition as diagonal partial shading and activates the corresponding switch to balance current across the diagonals of the block. If more than two modules have low irradiance, or if all modules display nearly uniform irradiance, the system determines that cross-linking is unnecessary and keeps the switch deactivated.

After evaluating all 2×2 blocks, the system updates each switch state within the MATLAB/Simulink model and dynamically adjusts the PV array configuration. The system then recalculates the current-voltage (I–V) and power-voltage (P–V) curves to determine maximum power output and overall efficiency. This method activates cross-ties only in shaded regions, thereby increasing power output without introducing additional control complexity or significant power losses.

The evaluation of configuration outcomes is based on four criteria: the global maximum power point (GMPP), the number of cross-tied interconnections, the fill factor (FF) as defined in Equation 24, and power losses (PL) as specified in Equation 25.

$$FF = \frac{GMPP}{V_{oc}\ x\ I_{SC}} \tag{24}$$

$$PL = GMPP\ (STC) - GMPP\ (PSC) \tag{25}$$

4. Results and Discussions

4.1 Mathematical Analysis

Under short-circuit conditions (zero total voltage), the value of the exponential term becomes negligible, and the effect of $\frac{\beta S_c}{S}$ on the I_{ph} of a single branch does not significantly influence the total current. Consequently, the total short-circuit current approaches the short-circuit current under unshaded conditions. The mathematical results in Equations 14 and 21 indicate the existence of a transition-point current, formulated as the break current, $I_{br} = 2I_{ph} - \frac{\beta S_c}{S}$. This value represents the current at which the I-V curve transitions to another peak. The I-V curve begins at the first knee point and breaks at I_{br}, forming a second peak and multiple maximum power points (MPPs) under both shading conditions.

The cross-tied interconnection automatically acts as a bypass current path, allowing part of the current from the unshaded string to flow laterally and compensate for node experiencing current deficiency. As a result, the total current at the array output terminal remains relatively stable even when one module experiences power reduction. In the second condition, each horizontal node receives a current proportional to the average irradiance along that path. Because the current difference between nodes is relatively small, the resulting cross-current is also small, leading to a more stable system.

The main difference lies in the presence of a logarithmic term within the exponential expression in Equation 15 for the cross-tied configuration, which acts as an indirect adaptive mechanism for mitigating total current reduction. This

logarithmic term represents the inter-string current coupling, meaning that the exponential term depends not only on the total voltage but also on the current distribution within the array, thereby damping the current reduction caused by shading. In contrast, Equation 16 for the Series–Parallel configuration contains an exponential term that depends solely on V_{total} without a logarithmic component. Consequently, current reduction occurs directly and proportionally with shading severity, making the total current more sensitive to the shaded module.

Equation 22 shows that in the cross-tied configuration, shading does not directly limit the entire string current because cross paths enable current redistribution between strings. Mathematically, this behavior is reflected by the logarithmic term and the implicit dependence of total current on the shading conditions, causing the current drop to become smaller and more distributed. In contrast, Equation 23 for the Series–Parallel configuration shows that shading on one module directly reduces the string current to the minimum current of the shaded module without any compensation mechanism: $2.\frac{\beta S_c}{S}.I_{ph}$. This behavior is indicated by the larger reduction in photocurrent and the explicit form of the equation, resulting in more significant power losses compared to the cross-tied configuration.

4.2 Simulation results

A 3×3 PV array configuration is used in this study, as presented in Table 2. A total of nine study cases were evaluated, consisting of three variations of partial shading conditions and a comparison between the PSO algorithm and the conventional P&O algorithm. Figures 4 and 5 illustrate the irradiance intensity patterns on the PV array, where the blue blocks (P11–P33) represent PV modules receiving full irradiance, while blocks with colour gradients and numerical values (e.g., 400 and 200 W/m²) indicate partial irradiance due to shading. All PV modules are assumed to have identical specifications to ensure consistency in the analysis. Regarding MPPT, the MPPT mechanism is beyond the scope of this study, as the primary focus is the array interconnection configuration. However, the mathematical analysis and simulation results indicate that the implementation of ON–OFF switches with cross-interconnection affects neighboring modules through current redistribution, and this effect is beneficial because it reduces current mismatch losses. In addition, the ACTI configuration produces a smoother P–V curve with fewer local peaks, thereby reducing the computational burden and improving the reliability of MPPT operation, as shown in the P–V characteristics results in Figure 7.

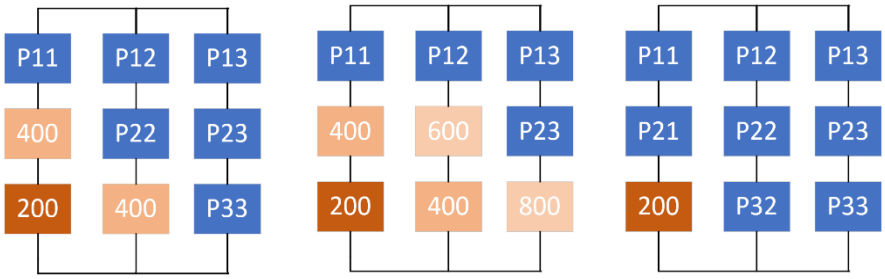

Figure 4. Series-Paralel Configuration

Figures 5 shows the PV array results with the ACTI reconfiguration technique, while the conventional Series-Parallel configuration is depicted in Figure 4. Each module within the string is equipped with an ON-OFF switch connected through cross-tied interconnection. When the PV module experiences reduced irradiance due to partial shading conditions, the corresponding interconnection switch is activated with the nearest string. Cross-tied interconnections are applied only in shaded regions; therefore, the ACTI technique adjusts the interconnection locations according to the shading pattern.

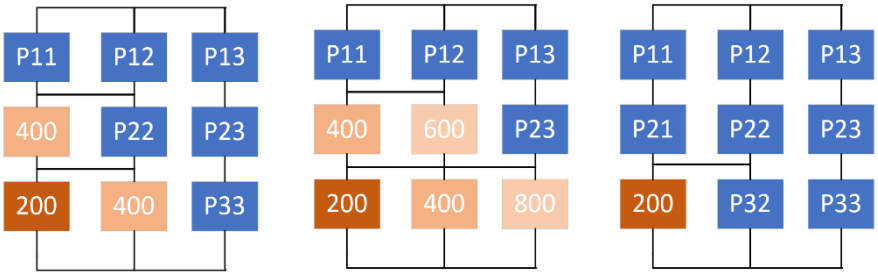

Figure 5. The optimal ACTI Reconfiguration

Table 2. The ACTI Reconfiguration Performance for 3×3 PV Array

Scenario (3×3 PV array)	The Power Output (Watt)	Power increase vs. SP (watt)	The number of cross-tied
Case 1 SP	87	-	0
Case 1 ACTI	120	33	2
Case 1 TCT	120	33	4
Case 2 SP	80	-	0
Case 2 ACTI	89	9	3
Case 2 TCT	89	9	4
Case 3 SP	92	-	0
Case 3 ACTI	134	42	1
Case 3 TCT	134	42	4

As shown in Table 2, the ACTI configuration consistently enhances power output compared to the Series–Parallel (SP) configuration and achieves power levels comparable to TCT across all partial shading scenarios, while using fewer cross-tied interconnections. In Cases 1 and 3, ACTI delivers the same power output as TCT despite utilizing only a fraction of the interconnection paths, indicating that selective placement of cross-tied interconnections is more effective than extensive wiring. These findings confirm that the power improvement achieved by ACTI results from efficient current redistribution, as supported by the mathematical analysis, thereby reducing system complexity without compromising performance.

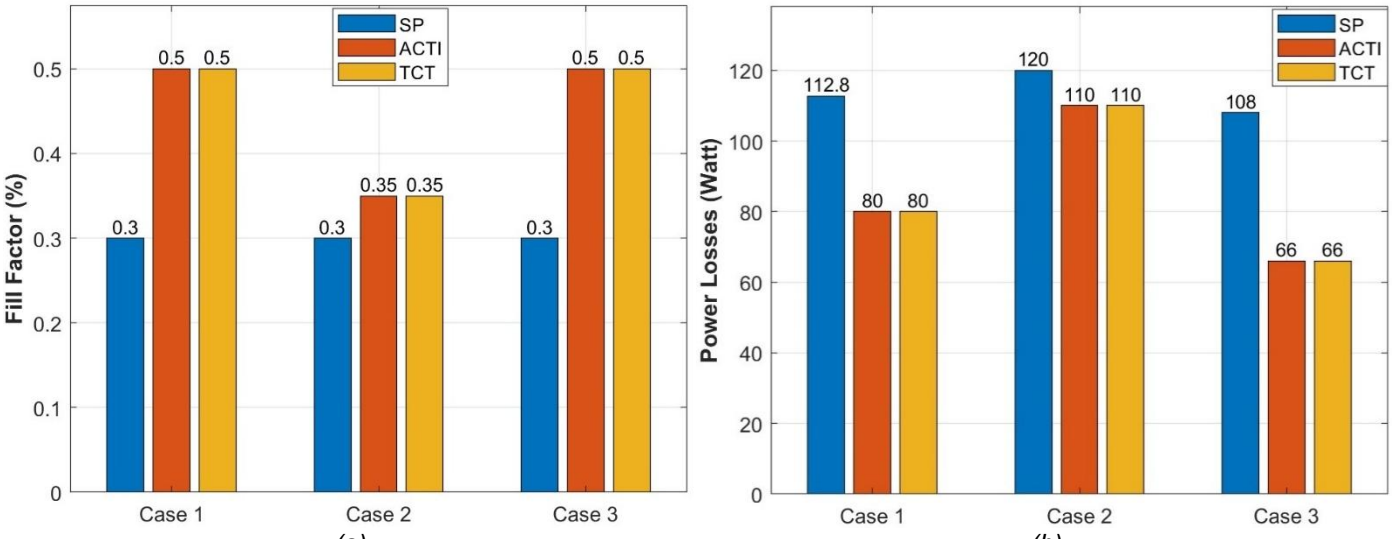

Figure 6. Indicator Performance for 3×3 PV Array: (a) Fill Factor and (b) Power Losses

As shown in Figures 6(a) and 6(b), the ACTI and TCT configurations consistently outperform the Series–Parallel (SP) configuration across all 3×3 PV array test scenarios. In Figure 6(a), the fill factor values for ACTI and TCT are higher than those for SP, indicating more ideal I–V curve characteristics and reduced current mismatch effects due to partial shading. This increase in fill factor directly correlates with the ability of both configurations to maintain more stable voltage and current levels. Furthermore, Figure 6(b) shows that the power losses in the ACTI and TCT configurations are significantly lower than those in the SP configuration across all cases, confirming the effectiveness of the current redistribution mechanism in reducing power losses caused by shaded modules. The comparable performance of ACTI and TCT across these two indicators demonstrates that selective cross-tied activation in ACTI is sufficient to achieve performance similar to TCT, while perserving the advantages of interconnection efficiency and reduced system complexity.

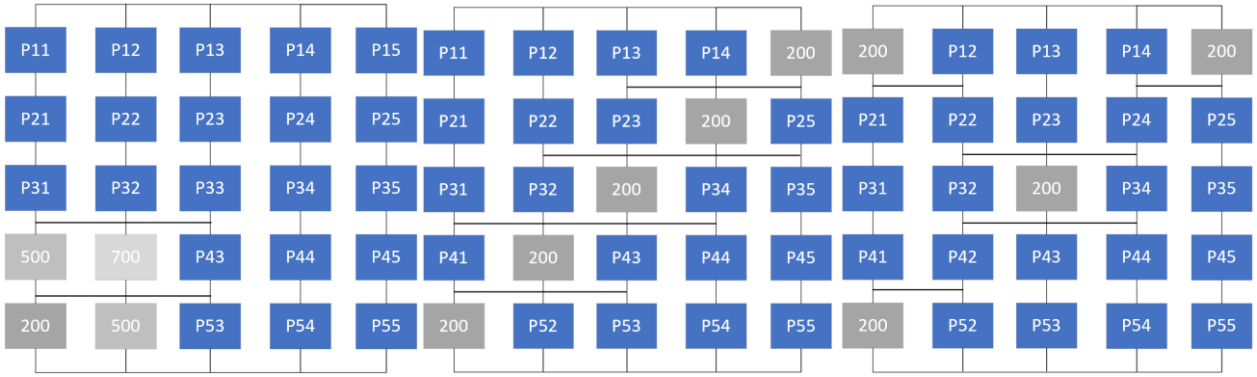

Figure 7. Partial Shading Patterns for 5×5 PV Array

Table 3 shows that the ACTI configuration consistently improves power output compared to the Series–Parallel (SP) configuration for a 5×5 PV array across all shading patterns, as illustrated in Figure 7, while achieving performance comparable to TCT with significantly fewer interconnections. For instance, under diagonal shading, power increases from 396 W (SP) to 420 W (ACTI) using 10 cross-tied interconnections, whereas TCT requires 16 cross-tied interconnections to achieve the same power level. In the case of random shading, ACTI increases power from 352 W to 374 W using only seven cross-tied interconnections, demonstrating that selective current redistribution can efficiently manage complex mismatches. These results confirm that ACTI adapts to shading patterns through optimized placement of cross-tied interconnections rather than extensive wiring, thereby providing meaningful and practical advantages for large-scale PV system implementation.

Table 3. The Result Performances of 5×5 PV Array

Scenario (5×5 PV array)	The Power Output (Watt)	An increase of power w.r.t sub-case a (watt)	The number of cross-tied
Corner Shading (SP)	384	-	0
Corner Shading (ACTI)	392	8	4
Corner Shading (TCT)	392	8	16
Diagonal Shading (SP)	396	-	0
Diagonal Shading (ACTI)	420	24	10
Diagonal Shading (TCT)	420	24	16
Random Shading (SP)	352	-	0
Random Shading (ACTI)	374	22	7
Random Shading (TCT)	374	22	16

In Figure 8(a) (corner shading), the P–V curves for SP and ACTI nearly overlap, indicating only a minor improvement because the shaded area is limited to the corners of the array and affects only a small number of modules. Conversely, in Figure 8(b) (diagonal shading), the ACTI curve appears more stable and exhibits only one dominant peak, whereas the SP curve shows two local peaks caused by current mismatches across the diagonals. This indicates that ACTI successfully balances current distribution by activating cross-tied switches in blocks experiencing different irradiance levels, thereby eliminating undesired local peaks and concentrating energy at the global maximum power point (GMPP). In Figure 8(c) (random shading), the ACTI curve is also smoother and exhibits a higher peak than the SP curve, demonstrating the effectiveness of the proposed system in stabilizing power output under random shading conditions.

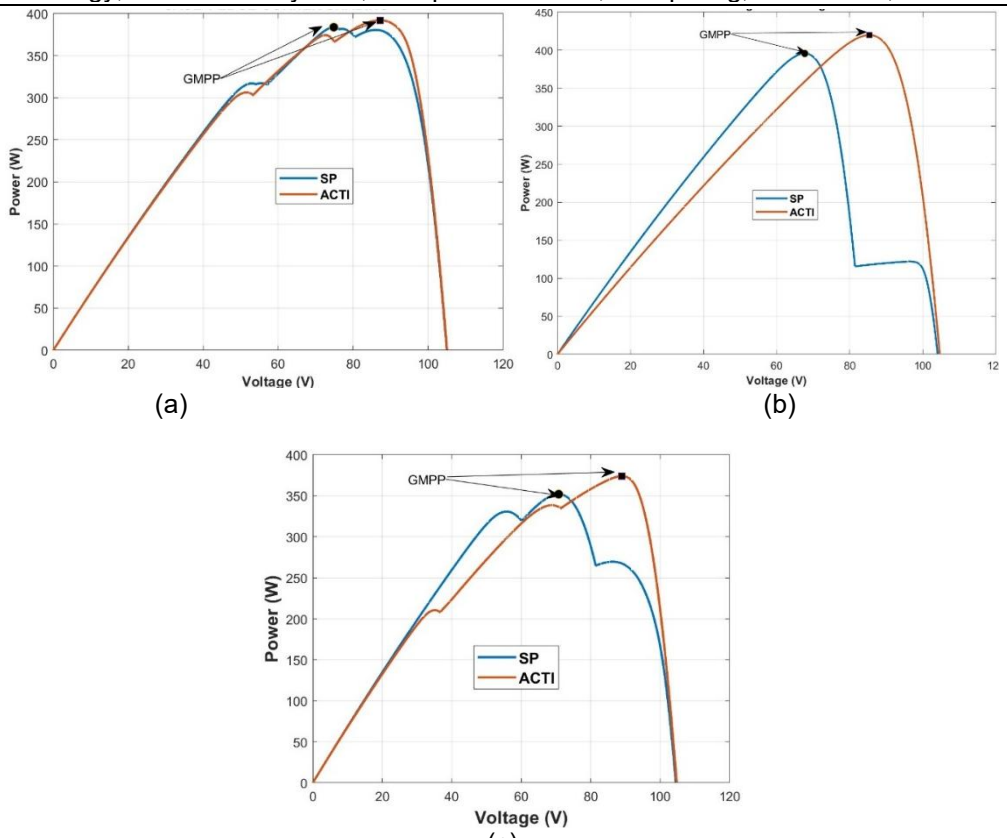

Figure 8. P-V Characteristic Curve Comparisons for 5×5 PV Array: (a) Corner Shading; (b) Diagonal Shading; (c) Random Shading

The main advantage of the proposed configuration is reflected in the shape of the power–voltage (P–V) curve, which becomes smoother and more concentrated. This condition facilitates the maximum power point (MPP) tracking process because the MPPT algorithm no longer needs to deal with multiple local peaks, as commonly observed in the Series–Parallel (SP) configuration. In the SP configuration, the presence of several power peaks often causes the MPPT algorithm to become trapped at a local maximum point. In contrast, ACTI simplifies the P–V characteristics through selective current redistribution, thereby reducing oscillations during the tracking process. In addition, ACTI activates cross-tied paths only in the regions of the array experiencing irradiance differences, enabling power improvement without excessively increasing circuit complexity. With this approach, ACTI maintains a balance between power enhancement, output stability, and interconnection simplicity, making it more practical and economical solution for static partial shading conditions. Thus, ACTI not only improves output power efficiency and MPPT stability but also provides a more adaptive, connection-efficient, and easily implementable configuration, making it a superior alternative for PV systems operating under non-uniform shading conditions.

Based on Table 4, the Series–Parallel (SP) configuration has the lowest implementation complexity and cost and is the most commonly used configuration. However, its performance decreases significantly under partial shading conditions because the most shaded module determines the string current. This condition results in severe current mismatch and reduced output power. Total Cross-Tied (TCT) and static reconfiguration techniques can generate higher power through current-sharing mechanisms, but both require numerous cross-ties interconnections and extensive wiring. Consequently, these configurations increase system complexity, installation cost, and poor scalability when applied to large PV arrays.

Meanwhile, AI-based dynamic adaptive reconfiguration techniques can achieve near-optimal power performance by dynamically reconfiguring modules. However, these techniques require highly complex switching and control systems and involve high implementation costs, making them less practical for long-term deployment. Among the available methods, Adaptive Cross-Tied Interconnection (ACTI) configuration offers the most balanced solution by delivering high power output with relatively low configuration complexity and minimal selective wiring. By activating cross-ties interconnections only in shaded areas, ACTI effectively reduces current mismatch without introducing significant hardware overhead, making it ideal for PV systems operating under static partial shading caused by buildings, trees, or other permanent objects.

Table 4. Comparison of PV Array Configuration Technique Under Partial Shading Conditions

Configuration Technique	Power Output under partial shading	Configuration complexity	Wiring requirement	Implementation cost	Practical remarks
Series – Parallel (SP) [7]	Low	Very simple	Minimal	Cheap	Widely used but highly sensitive to shading; severe current mismatch limits power output
Total Cross-Tied (TCT)	High	Complex	A large number of cross-ties	Expensive	Effective current sharing but poor scalability due to excessive wiring
Static reconfiguration [26]	High	Very complex	A large number of cross-ties	Expensive	Effective current sharing but poor scalability due to complex wiring
Adaptive Cross-Tied Interconnection (ACTI)	High	Simple-moderate	Minimal and selective	Cheap	Optimal trade-off between efficiency and simplicity; suitable for static partial shading
Dynamic Adaptive Reconfiguration (AI – based) [27], [28], [29], [30], [31]	High	Very complex	Very large (module-level switching)	Very expensive	Near-optimal performance but impractical for large systems due to hardware and control overhead

The Adaptive Cross-Tied Interconnection (ACTI) configuration provides a more balanced solution for static partial shading conditions. ACTI can achieve high power output with minimal and selective wiring because cross-ties interconnections are activated only in areas genuinely experience shading. These characteristics make ACTI particularly suitable for PV installations in urban environments or areas with permanent structures, where shading patterns are relatively fixed and do not require continuous global reconfiguration. In contrast, AI-based adaptive dynamic reconfiguration techniques may achieve near-optimal power performance but require highly complex switching and control infrastructures, resulting in higher implementation costs and reduced practicality. Under static shading conditions, such approaches are less efficient and more difficult to implement, making ACTI a more practical, economical, and easily deployable solution.

5. Conclusion

This research aimed to develop a photovoltaic array configuration with a strong mathematical basis and practical feasibility to enhance power extraction under partial shading conditions without increasing wiring or control system complexity. Based on the analytical formulations and MATLAB/Simulink simulation results, it can be concluded that Adaptive Cross-Tied Interconnection (ACTI) configuration successfully achieves this objective by reducing current mismatches through a selective current redistribution mechanism, resulting in more stable current-voltage characteristic of the array. Quantitatively, in a 3×3 PV array, ACTI increases power output by up to 48% compared to the Series-Parallel configuration. Meanwhile, in a 5×5 PV array, the efficiency improvement ranges from 2% to 6%, depending on the shading pattern. From an implementation perspective, ACTI shows power performance comparable to a full Total Cross-Tied (TCT) configuration while requiring a significantly smaller number of interconnections, thereby achieving the intended balance between efficiency improvements and implementation simplicity. In addition, the smoother power-voltage curve indicates that ACTI can improve the reliability of achieving the global maximum power point. Overall, ACTI is an efficient, economical, and mathematically validated solution for improving the performance of PV systems under non-uniform irradiation conditions, especially in cases of static or semi-static partial shading.

Acknowledgement

This research was funded by the Hi-Ma Research Grant from Universitas Islam Malang. The authors would also like to express their sincere appreciation to the Department of Electrical Engineering, Faculty of Electrical and Electronics Engineering, Universiti Tun Hussein Onn Malaysia, Johor, Malaysia, for the valuable collaboration and technical support provided throughout this study.

References

[1] M. Farghali *et al.*, "Strategies to save energy in the context of the energy crisis: a review," *Environ. Chem. Lett.*, vol. 21, no. 4, pp. 2003–2039, 2023. https://doi.org/10.1007/s10311-023-01591-5

[2] N. A. Pambudi *et al.*, "Renewable Energy in Indonesia: Current Status, Potential, and Future Development," *Sustainability*, vol. 15, no. 3, 2023. https://doi.org/10.3390/su15032342

[3] E. Kabir, P. Kumar, S. Kumar, A. A. Adelodun, and K.-H. Kim, "Solar energy: Potential and future prospects," *Renewable and Sustainable Energy Reviews*, vol. 82, pp. 894–900, 2018. https://doi.org/10.1016/j.rser.2017.09.094

[4] M. J. Afroni, E. S. Wirateruna, and O. Melfazen, "An Experimental Study of Partial Shading Effects on the P-V Characteristic Curve," in *2022 11th Electrical Power, Electronics, Communications, Controls and Informatics Seminar (EECCIS)*, 2022, pp. 22–27. https://doi.org/10.1109/EECCIS54468.2022.9902950

[5] S. M. Maharana, A. Mohapatra, C. Saiprakash, and A. Kundu, "Performance Analysis of Different PV Array Configurations under Partial Shading Condition," in *2020 International Conference on Computational Intelligence for Smart Power System and Sustainable Energy (CISPSSE)*, 2020, pp. 1–5. https://doi.org/10.1109/CISPSSE49931.2020.9212244

[6] E. S. Wirateruna, M. J. Afroni, and F. Badri, "Design of Maximum Power Point Tracking Photovoltaic System Based on Incremental Conductance Algorithm using Arduino Uno and Boost Converter ," *Applied Technology and Computing Science Journal*, vol. 4, no. 2, pp. 101–112, 2022.

[7] C. V Chandrakant and S. Mikkili, "A Typical Review on Static Reconfiguration Strategies in Photovoltaic Array Under Non-Uniform Shading Conditions," *CSEE Journal of Power and Energy Systems*, vol. 9, no. 6, pp. 2018–2039, 2023. https://doi.org/10.17775/CSEEJPES.2020.02520

[8] V. C. Chavan, S. Mikkili, and T. Senjyu, "Experimental Validation of Novel Shade Dispersion PV Reconfiguration Technique to Enhance Maximum Power Under PSCs," *CPSS Transactions on Power Electronics and Applications*, vol. 8, no. 2, pp. 137–147, Jun. 2023. https://doi.org/10.24295/CPSSTPEA.2023.00014

[9] A. A. Desai and S. Mikkili, "Modelling and analysis of PV configurations (alternate TCT-BL, total cross tied, series, series parallel, bridge linked and honey comb) to extract maximum power under partial shading conditions," *CSEE Journal of Power and Energy Systems*, vol. PP, no. 99, 2019. https://doi.org/10.17775/CSEEJPES.2020.00900

[10] H. Oufettoul, S. Motahhir, G. Aniba, M. Masud, and M. A. AlZain, "Improved TCT topology for shaded photovoltaic arrays," *Energy Reports*, vol. 8, pp. 5943–5956, 2022. https://doi.org/10.1016/j.egyr.2022.04.042

[11] C. W. Priananda, A. Rajagukguk, D. C. Riawan, Soedibyo, and M. Ashari, "New approach of maximum power point tracking for static miniature photovoltaic farm under partially shaded condition based on new cluster topology," in *2017 15th International Conference on Quality in Research (QiR) : International Symposium on Electrical and Computer Engineering*, 2017, pp. 444–449. https://doi.org/10.1109/QIR.2017.8168527

[12] A. Rajagukguk, C. W. Priananda, D. C. Riawan, Soedibyo, and M. Ashari, "Novel derivative cluster area methods (DCAM) for power optimization of PV farm under dinamically shading effect," in *2017 15th International Conference on Quality in Research (QiR) : International Symposium on Electrical and Computer Engineering*, 2017, pp. 434–438. https://doi.org/10.1109/QIR.2017.8168525

[13] M. J. Afroni and E. S. Wirateruna, "4 Section method for MPPT optimization in Solar Panel Experiments under PSC v221023," in *2023 International Conference on Smart-Green Technology in Electrical and Information Systems (ICSGTEIS)*, 2023, pp. 172–177. https://doi.org/10.1109/ICSGTEIS60500.2023.10424047

[14] E. S. Wirateruna and A. F. A. Millenia, "Design of MPPT PV using Particle Swarm Optimization Algorithm under Partial Shading Condition," *International Journal of Artificial Intelligence & Robotics (IJAIR)*, vol. 4, no. 1, pp. 24–30, May 2022. https://doi.org/10.25139/ijair.v4i1.4327

[15] P. Murugesan, P. Winston David, P. Murugesan, and N. Kalyani Solaisamy, "One-step adaptive reconfiguration technique for partial shaded photovoltaic array," *Solar Energy*, vol. 263, p. 111949, 2023. https://doi.org/10.1016/j.solener.2023.111949

[16] E. S. Wirateruna, M. Ashari, and D. C. Riawan, "Estimation and Assessment of Partial Shading Patterns in Large PV Farms Using ANN Algorithm," *IEEE Access*, vol. 13, pp. 139189–139202, 2025. https://doi.org/10.1109/ACCESS.2025.3596268

[17] J. H. Teng, H. C. Wu, Z. H. Wu, and W. H. Huang, "Efficient Partial Shading Detection for Photovoltaic Generation Systems," *IEEE Trans. Sustain. Energy*, vol. 14, no. 4, pp. 2249–2259, Oct. 2023. https://doi.org/10.1109/TSTE.2023.3271298

[18] D. S. Pillai, J. P. Ram, A. M. Y. M. Ghias, M. A. Mahmud, and N. Rajasekar, "An Accurate, Shade Detection-Based Hybrid Maximum Power Point Tracking Approach for PV Systems," *IEEE Trans. Power Electron.*, vol. 35, no. 6, pp. 6594–6608, Jun. 2020. https://doi.org/10.1109/TPEL.2019.2953242

[19] T. S. Babu, D. Yousri, and K. Balasubramanian, "Photovoltaic Array Reconfiguration System for Maximizing the Harvested Power Using Population-Based Algorithms," *IEEE Access*, vol. 8, pp. 109608–109624, 2020. https://doi.org/10.1109/ACCESS.2020.3000988

[20] D. Yousri, S. B. Thanikanti, K. Balasubramanian, A. Osama, and A. Fathy, "Multi-Objective Grey Wolf Optimizer for Optimal Design of Switching Matrix for Shaded PV array Dynamic Reconfiguration," *IEEE Access*, vol. 8, pp. 159931–159946, 2020. https://doi.org/10.1109/ACCESS.2020.3018722

[21] T. S. Babu, J. P. Ram, T. Dragičević, M. Miyatake, F. Blaabjerg, and N. Rajasekar, "Particle Swarm Optimization Based Solar PV Array Reconfiguration of the Maximum Power Extraction Under Partial Shading Conditions," *IEEE Trans. Sustain. Energy*, vol. 9, no. 1, pp. 74–85, 2018. https://doi.org/10.1109/TSTE.2017.2714905

[22] B. Aljafari, P. R. Satpathy, and S. B. Thanikanti, "Partial shading mitigation in PV arrays through dragonfly algorithm based dynamic reconfiguration," *Energy*, vol. 257, p. 124795, 2022. https://doi.org/10.1016/j.energy.2022.124795

[23] X. Zhang, D. Meng, W. Li, T. Yu, Z. Fan, and Z. Hao, "Evolutionary based Pareto optimization algorithms for bi-objective PV array reconfiguration under partial shading conditions," *Energy Convers. Manag.*, vol. 271, p. 116308, 2022. https://doi.org/10.1016/j.enconman.2022.116308

[24] A. A. Teyabeen, N. B. Elhatmi, A. A. Essnid, and A. E. Jwaid, "Parameters Estimation of Solar PV Modules Based on Single-Diode Model," in *2020 11th International Renewable Energy Congress (IREC)*, 2020, pp. 1–6. https://doi.org/10.1109/IREC48820.2020.9310365

[25] A. Alhejab, M. Abbasi, and S. Ahmed, "A Single Voltage Sensor Bypass Switch-Based Photovoltaic Fault Localization," *IEEE J. Photovolt.*, pp. 1–11, 2025. https://doi.org/10.1109/JPHOTOV.2025.3530001

[26] V. Gautam, S. Khatoon, and M. F. Jalil, "A Review on Various Mathematical Based Static Reconfiguration Strategies to Improve Generated Power under Partial Shading Conditions," in *2023 International Conference on Recent Advances in Electrical, Electronics & Digital Healthcare Technologies (REEDCON)*, 2023, pp. 25–30. https://doi.org/10.1109/REEDCON57544.2023.10150794

[27] K. Osmani, A. Haddad, H. Jaber, T. Lemenand, B. Castanier, and M. Ramadan, "Mitigating the effects of partial shading on PV system's performance through PV array reconfiguration: A review," *Thermal Science and Engineering Progress*, vol. 31, p. 101280, 2022. https://doi.org/10.1016/j.tsep.2022.101280

[28] M. Jalal, I. U. Khalil, A. U. Haq, A. Flah, and S. A. M. Abdel Wahab, "Advancements in PV Array Reconfiguration Techniques: Review Article," *IEEE Access*, vol. 12, pp. 183751–183778, 2024. https://doi.org/10.1109/ACCESS.2024.3509955

[29] B. Yang, “Genetic Algorithm Based PV Array Reconfiguration Technique under Partial Shading Condition,” in *2023 IEEE International Conference on Power Science and Technology (ICPST)*, 2023, pp. 498–502. https://doi.org/10.1109/ICPST56889.2023.10164934

[30] V. K. Yadav, A. D. Behera, R. Singh, A. Maheshwari, S. Ghosh, and A. Prakash, “A novel PV array reconfiguration technique based on circular array data structure,” *Energy*, vol. 283, p. 128505, 2023. https://doi.org/10.1016/j.energy.2023.128505

[31] S. Saravanan, R. S. Kumar, and P. Balakumar, “Binary firefly algorithm based reconfiguration for maximum power extraction under partial shading and machine learning approach for fault detection in solar PV arrays,” *Appl. Soft Comput.*, vol. 154, Mar. 2024. https://doi.org/10.1016/j.asoc.2024.111318